Energy Conversion and Management 82 (2014) 71–82

Contents lists available at ScienceDirect

Energy Conversion and Management

journal homepage: www.elsevier.com/locate/enconman

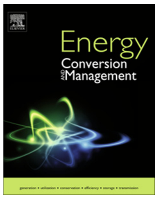

Characterization of lignocellulosic biomass thermal degradation and physiochemical structure: Effects of demineralization by diverse acid solutions

Masoud Asadieraghi [a,b], Wan Mohd Ashri Wan Daud [a,*]

[a] Department of Chemical Engineering, Faculty of Engineering, University of Malaya, 50603 Kuala Lumpur, Malaysia
[b] Arak Research Center, Petrochemical Research and Technology Company, National Petrochemical Company, No. 27, Sarv Alley, Shirazi-south, Mollasadra, P.O. Box 1435884711, Tehran, Iran

ARTICLE INFO

Article history:
Received 2 December 2013
Accepted 1 March 2014
Available online 22 March 2014

Keywords:
Palm oil biomass
Demineralization
TGA-MS
TGA-FTIR
Pyrolysis
Physiochemical structure

ABSTRACT

To eliminate the negative impacts of inorganic constituents during biomass thermochemical processes, leaching method by different diluted acid solutions was chosen. The different palm oil biomass samples (palm kernel shell (PKS), empty fruit bunches (EFB) and palm mesocarp fiber (PMF)) were pretreated by various diluted acid solutions (H_2SO_4, $HClO_4$, HF, HNO_3, HCl). Acids with the highest degrees of demineralization were selected to investigate the dematerialization impacts on the biomass thermal characteristics and physiochemical structure. Thermogravimetric analysis coupled with mass spectroscopy (TGA-MS) and Fourier transform infrared spectroscopy (TGA-FTIR) were employed to examine the biomass thermal degradation. TGA and DTG (Derivative thermogravimetry) indicated that the maximum degradation temperatures increased after acid pretreatment due to the minerals catalytic effects. The main permanent evolved gases comprising H_2, CO_2, CO were detected online during analysis. The major permanent gases produced at the temperature range of 250–750 °C were attributed to the condensable vapors cracking and probably some secondary reactions. The physiochemical structure change of the acid-treated biomass samples was examined by using Brunauer Emmett Teller (BET) method, Scanning Electron Microscope (SEM) and FTIR. The pyrolysis kinetics of the different palm oil biomasses were investigated using first order reaction model.

© 2014 Elsevier Ltd. All rights reserved.

1. Introduction

Depletion of fossil fuel resources and environmental issues associated with the CO_2 accumulations in the atmosphere are the main reasons increasing the attentions toward renewable energy resources like biomass.

Various thermochemical technologies (pyrolysis, torrefaction, gasification, etc.) can be utilized to convert the biomass to the bio-oil. Among them, pyrolysis is a remarkable and most known industrial technology used for the bio-oil production. Pyrolysis can be defined as the conversion of the biomass to liquid bio-oil, solid charcoal and gaseous products in the absence of oxygen under atmospheric pressure and moderate temperature ranging from 300 to 600 °C [1]. The major constituents of the biomass are cellulose, hemicelluloses, lignin, inorganic and some extractives, which have different thermal behavior during pyrolysis [2,3].

Thermal gravimetric analysis (TGA) and derivative thermogravimetry (DTG) have been utilized by different researchers to investigate the biomass pyrolytic behavior and kinetics [3–7]. TGA coupled with mass spectrometry (MS) and infrared spectroscopy (FTIR) provides the conditions for real-time (online) quantitative and qualitative evolved gas analysis, respectively. The utilization of MS and FTIR techniques along with thermal analysis can facilitate a deeper insight of the kinetic scheme and consequently to understanding the actual reaction mechanism [8,9]. Several investigations on the biomass thermal analysis have been carried out using integrated TGA-MS [10–12].

The effects of inorganic metals on thermal degradation of the lignocellulosic biomass have been intensively studied by researchers [13–17]. They mostly concluded that, the presence of alkaline and alkaline earth metallic species (K, Na, Mg, and Ca) can influence the quality and quantity of the pyrolysis and gasification products. Commonly, inorganic species are maintained on the char

---

* Corresponding author. Tel.: +60 172907256; fax: +60 10379675371.
E-mail addresses: masoud.asadieraghi@gmail.com (M. Asadieraghi), ashri@um.edu.my (W.M.A. Wan Daud).

http://dx.doi.org/10.1016/j.enconman.2014.03.007
0196-8904/© 2014 Elsevier Ltd. All rights reserved.

surface instead of being volatized during pyrolysis process. Therefore, they can catalyze the biomass conversion and char formation reaction [18,19]. The high inorganic constituents in the bio-oil, originated from the biomass having high quantity of minerals, can catalyze polymerization reaction during the bio-oil storage and led to its viscosity increase [20], whereas their removal from the biomass before pyrolysis can increase the bio-oil yield and stability [21].

Biomass demineralization with acid solutions had been indicated to be a suitable method to remove inorganic constituents from the biomass, and to improve its fuel properties. So, various leaching experiments using diverse conventional acid solutions including hydrochloric acid, sulfuric acid, hydrofluoric acid, perchloric acid, nitric acid et al. were conducted [17,19,22–24].

Biomass pretreatment using acid solution before pyrolysis can eliminate the needs for additional fractionation step. This advantage can facilitate a considerable simplification of the process and large scale bio-oil production, as well as extensive reduction of energy consumption and cost of pyrolysis [24]. Furthermore, minerals elimination from the used acid solution (recovery) and its recycling to the pretreatment stage can enhance process economy and make it environment-friendly.

TGA/DTG investigations carried out by Müller-Hagedorn et al. [25] showed the doped biomass with inorganic spices (Na, K and Ca) shifted DTG curves to lower temperature compared with washed and untreated biomass. Further, it was proved that the doped biomass with potassium decreased activation energy compared to that of washed one [26]. As mentioned, several researches available in the literatures have focused on the effects of inorganics on the biomass behavior, but only a few investigations on the leaching process effects on the biomass physiochemical structure [17,23] have been reported. To the best of our knowledge, no published study has been reported on the effects of minerals removal (using acid solutions) on the palm oil biomasses thermal degradation and physiochemical structure.

This study is aiming to find the most efficient acid solutions to leach out the minerals from the biomass samples and to investigate the impacts of these diluted acids on the physiochemical structure and thermal behavior of the palm oil biomasses. In this regard, the different palm oil biomass samples (PKS, EFB and PMF) were pretreated by H_2SO_4, $HClO_4$, HF, HNO_3 and HCl diluted solutions to remove inorganic species through leaching process. Consequently, the treated samples with the highest degree of ash removal were profoundly analyzed to measure the demineralization efficiency and the effects of deashing process on the thermal degradation and the physiochemical structure of the biomasses. TGA-MS and TGA-FTIR were employed to study the pyrolysis characteristics, evolved permanent gases products distribution and reaction kinetics.

2. Materials and methods

2.1. Biomass materials

The palm oil biomasses comprising palm kernel shell (PKS), empty fruit bunches (EFB) and palm mesocarp fiber (PMF) were obtained from Szetech Engineering Sdn. Bhd. located in Selangor, Malaysia. The samples were crushed using high-speed rotary cutting mill and sieved to desired particle size (<300 μm). Then, the samples were dried at 105 °C for 24 h and kept in tightly screw cap plastic bottles.

2.2. Demineralization pretreatments

Different types of the dried palm oil biomasses (PKS, EFB and PMF) were subjected to diverse diluted acid solutions (H_2SO_4 (96 wt.%), $HClO_4$(70 wt.%), HF(49 wt.%), HNO_3(65 wt.%), HCl (37 wt.%)), all supplied by R&M Chemicals, for the purpose of inorganics removal. Acid washing pretreatment process aimed to maximize the ash extraction through leaching process. For this purpose, 20 g of the biomass samples were treated by 2.0 M acid solutions at room temperature for 48 h and then filtered and washed with distilled water. The ratio of the acid solutions to the biomass samples was considered as 15 (g solution/g biomass). The washing process was continued to a constant pH value. The leached biomass samples were dried in oven at 105 °C over 24 h and kept in tightly screw cap bottles.

2.3. Biomasses proximate and ultimate analysis

Proximate analysis was carried out by utilizing thermogravimetric analysis. Volatile matter, fixed carbon and moisture contents were measured according to ASTM D-5142-02a using TGA/Q500 manufactured by TA Instruments. Ash content of the biomasses samples was determined by their ignition in a muffle furnace at 575 °C for 24 h according to ASTM E-1755-01 standard method. Ash content (wt.%) was calculated by dividing ash weight to initial weight of dried biomass sample at 105 °C.

Ultimate analysis was carried out to determine the basic elemental composition of the biomass samples. The samples' ultimate analysis was done using a Perkin–Elmer model 2400, Series II CHNS/O analyzer to measure carbon, hydrogen, nitrogen and sulfur contents. Oxygen content was then calculated by difference. Higher heating value (HHV) was calculated from the elemental compositions using Eq. (1) from Channiwala and Parikh [27]:

$$\mathrm{HHV}\left(\frac{\mathrm{MJ}}{\mathrm{kg}}\right) = 0.3491\mathrm{C} + 1.1783\mathrm{H} + 0.1005\mathrm{S} - 0.1034\mathrm{O} - 0.0151\mathrm{N} - 0.0211\mathrm{A} \quad (1)$$

where C, H, N, O, S and A represents carbon, hydrogen, nitrogen, oxygen, sulfur and ash contents of materials, respectively, expressed in dry basis weight percentage.

2.4. X-ray Flouresence (XRF) analysis

All the biomass samples inorganic contents were quantified using X-ray Flouresence (XRF) instrument (PANalytical Axios$^{\mathrm{mAX}}$).

2.5. Scanning Electron Microscopy (SEM) analysis

The surface nature of the virgin and treated samples was investigated by SEM (model FEI QUANTA 450 FEG, operating at a 5 kV accelerating voltage and low vacuum) to characterize the effects of leaching process on the physical structure of the biomasses. Conductive coating was not applied to prepare the samples for SEM analysis. Samples were prepared by their sticking on carbon sheet.

2.6. Surface area and porosity analysis

The surface area and pore size of the samples were measured, using nitrogen ($N_{2)}$ adsorption/ desorption isotherm at −196 °C, by the Micrometrics ASAP 2020 gas adsorption analyzer. All the samples were degassed in vacuum at 130 °C for 24 h before the measurement. Filler rod was used in the sample tube due to low surface area of samples. Estimation of pore size diameter was done by Barrett–Joyner–Halenda (BJH) method.

2.7. FTIR spectroscopy

To qualitatively analyze the functional groups of chemical components available in the virgin and pretreated biomass samples, Fourier transform infrared spectroscopy (FTIR; model: BRUKER TENSOR 27) was utilized. The samples were scanned over the range from 600 to 4000 cm^{-1} with a resolution of 4 cm^{-1}.

2.8. TGA-MS, TGA-FTIR experiments

TGA-MS and TGA-FTIR analysis were carried out by simultaneous thermal analyzers (TA Instruments Q500 and NETZSCH STA 449/F3) coupled with MS type (PFEIFFER Vacuum-Thermostar TM) and FTIR type (BRUKER TGA-IR), respectively. Pure Nitrogen (99.999%) was used as carrier gas in all experiments. In order to prevent unnecessary evolved gas (like tar and etc.) condensation in both assemblies, a skimmer coupling system was employed while the connected capillary tube between TGA and evolved gas analyzers (MS and FTIR) were kept at 200 °C. To minimize the effects of heat and mass transfer limitations during the samples analysis, the samples quantity was selected approximately 5 mg with the particle size less than 300 μm at pure nitrogen flow rate of 150 ml/min. The samples loaded to alumina crucible pan were heated from 35 °C to 850 °C at heating rate of 15 °C/min.

Mass spectrometer worked with electron ionization energy of 70 eV and provided mass spectra up to 300 a.m.u, while FTIR online gas analysis was recorded from 4000 to 400 cm^{-1}. MS spectra corresponded to 2, 28, 44 a.m.u. indicated the release of main pyrolysis gases H_2, CO, and CO_2, respectively [28].

2.9. Biomass pyrolysis reaction kinetics

The solid state biomass pyrolysis kinetics using various mathematical and methodological models have been investigated by several researchers [29]. Eq. (2) shows the general rate equation as:

$$\frac{dx}{dt} = kf(x) \tag{2}$$

where x is the conversion degree of the biomass feedstock expressed in Eq. (3), k is the reaction rate constant and $f(x)$ refers to a selected model of reaction mechanism.

$$x = \frac{m_0 - m_t}{m_0 - m_f} \tag{3}$$

where m_t is corresponded to the sample mass at time t, m_0 and m_f are initial and final mass of biomass, respectively. The reaction rate constant can be obtained from Arrhenius equation as Eq. (4).

$$k = k_0 \exp\left(\frac{-E_a}{RT}\right) \tag{4}$$

where k_0 is rate constant pre-exponential factor, E_a, R and T are activation energy (Kj/mol), universal gas constant (8.314 J/mol K), and temperature (K), respectively. Furthermore, the reaction model expressed in Eq. (2) can be defined as Eq. (5).

$$f(x) = (1 - x)^n \tag{5}$$

where n is the reaction order. According to the literature [7,10,29], in many applications, the biomass pyrolysis was assumed to be a reaction with first order ($n = 1$).

For a constant pyrolysis heating rate of β, $\beta = dT/dt$, rearrangement of Eq. (2) and its integration by using the Coats-Redfern method [30] conducted to Eq. (6).

$$\ln\left[-\frac{\ln(1-x)}{T^2}\right] = \ln\left[\frac{k_0 R}{\beta E_a}\left(1 - \frac{2RT}{E_a}\right)\right] - \frac{E_a}{RT} \tag{6}$$

In Eq. (6), the value of $2RT/E_a \ll 1$ [31] therefore, it can be simplified to:

$$\ln\left[-\frac{\ln(1-x)}{T^2}\right] = \ln\left[\frac{k_0 R}{\beta E_A}\right] - \frac{E_a}{RT} \tag{7}$$

Thus, the plot of $\ln[-\ln(1-x)/T^2]$ versus $1/T$ is a linear line with the slope and intercept of $-E_a/R$ and $\ln[k_0 R/\beta E_a]$, respectively. Accordingly, the pre-exponential factor (k_0) and activation energy (E_a) can be determined.

3. Results and discussion

3.1. Basic characterization of the biomass samples

Fig. 1 shows the ash content of the virgin and pretreated palm oil biomass samples. The biomasses ultimate/proximate analysis and their inorganic constituents (before and after demineralization) are summarized in Tables 1 and 2, respectively. Compared to the virgin samples, a significant ash removal from EFB (7% to 0.43%) and PMF (8.4% to 1.35%) was performed by HF diluted solution, while PKS-HF indicated more resistance to ash elimination. The maximum ash removal from PKS (16.3% to 4.6%) was observed when diluted acid leaching process was carried out by HCl. Different ash removal from the biomasses using same acid solution was possibly due to the inorganic contents (Table 2), nature, composition and structure of the various lignocellulosic biomass samples. Biomass virgin samples indicated various lignocellulosic contents (wt.%) [32]: PKS (20.8% cellulose, 22.7% hemicellolose and 50.7% lignin), EFB (38.3% cellulose, 35.8% hemicellolose and 22.1% lignin), and PMF (34.5% cellulose, 31.8% hemicellolose and 25.7% lignin). As can be observed, the cellulose and hemicellulose content of EFB was greater than that of PMF and PKS. On the other hand, PKS showed the highest lignin content. EFB and PMF indicated relatively similar lingocellulosic compositions and mineral contents (Table 2), whereas PKS showed completely different inorganics and lingocellulosic contents compared with EFB and PMF.

Proximate analysis of the biomass samples (with maximum ash removal) can be seen in Table 1. While the ash contents of the samples remarkably decreased, their volatile contents increased after leaching process. This could be led to the improvement of the biomass fuel properties like heat value. Also, ash removal from the biomasses could prevent the severe problems associated with the presence of high inorganic contents such as slagging, agglomeration, deposition and heated side corrosion in the thermochemical processes [23].

The biomass organic compounds are different oxygenated hydrocarbons which their major constituents are carbon, oxygen and hydrogen. The molecular mass of carbon is much heavier than hydrogen therefore; H/C wt.% ratio could reflect the amount of hydrocarbon components [33]. Removal of hydrocarbons during leaching process will be conducted to the H/C ratio enhancement. As can be seen in Table 1, the H/C wt.% elemental ratio in PKS-HCl, EFB-HF and PMF-HF slightly increased. This could specify that the

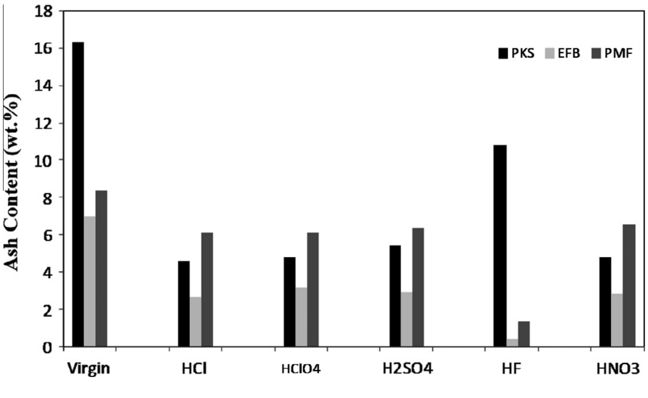

Fig. 1. Ash content of the different untreated and treated palm oil biomasses.

Table 1
Proximate and ultimate analysis of the virgin and demineralized palm oil biomasses (PKS, EFB and PMF).

Biomass	Moisture	Volatile Matters	Fixed Carbon	Ash					
Proximate analysis (wt.%)									
PKS	2.8	67.9	13.0	16.3					
EFB	6.3	79.2	7.5	7.0					
PMF	5.8	70.8	15.0	8.4					
PKS-HCl	5	72.8	17.6	4.6					
EFB-HF	5	82.0	12.57	0.43					
PMF-HF	5.3	81.7	11.65	1.35					
Ultimate analysis (wt.%)									
Acid	Biomass	Carbon	Hydrogen	Nitrogen	Sulphur	Oxygen[a]	H/C[b]	O/C[c]	HHV (MJ/kg)
–	PKS	49.05	5.59	0.76	0.38	44.60	0.114	0.909	16.1
	EFB	44.84	5.81	1.41	0.40	47.94	0.129	1.069	16.2
	PMF	47.76	5.59	2.13	0.49	44.52	0.117	0.932	17.0
HCl	PKS	49.79	5.89	0.77	0.38	43.55	0.118	0.874	18.8
	EFB	46.32	6.55	1.27	0.44	45.86	0.141	0.990	18.5
	PMF	47.68	6.39	2.06	0.47	43.87	0.134	0.920	18.3
$HClO_4$	PKS	50.03	6.14	0.79	0.33	43.04	0.122	0.860	19.2
	EFB	47.34	6.48	1.5	0.42	44.68	0.137	0.943	18.8
	PMF	48.18	6.31	2.1	0.43	43.41	0.131	0.901	18.4
H_2SO_4	PKS	48.48	6.06	0.79	0.35	44.67	0.125	0.921	18.3
	EFB	47.2	6.38	1.36	0.42	45.06	0.135	0.954	18.7
	PMF	48.16	6.35	1.93	0.43	43.56	0.132	0.904	18.4
HF	PKS	47.37	5.84	0.89	0.34	45.9	0.123	0.969	16.3
	EFB	46.9	6.31	1.59	0.36	45.38	0.131	0.967	19.0
	PMF	47.92	5.69	2.29	0.39	44.10	0.119	0.920	18.5
HNO_3	PKS	47.93	6.02	1.07	0.30	44.98	0.125	0.938	18.2
	EFB	45.48	6.12	2.42	0.34	45.98	0.134	1.011	17.7
	PMF	46.68	6.12	3.01	0.37	44.19	0.131	0.946	17.6

[a] By difference.
[b] Hydrogen/Carbon ratio.
[c] Oxygen/Carbon ratio.

Table 2
Biomass samples inorganic contents before and after pretreatment (wt.%) (XRF results).

Biomass samples	Al_2O_3	CaO	Fe_2O_3	K_2O	MgO	Na_2O	P_2O_5	SiO_2	ZnO
PKS Virgin	2.10	71.57	4.89	1.29	1.77	0.32	0.98	16.46	0.02
EFB Virgin	0.77	15.52	5.78	39.98	3.68	0.23	4.29	19.24	0.32
PMF Virgin	2.71	20.83	9.67	15.55	4.20	0.25	6.76	26.05	0.30
PKS-HCl	9.67	1.27	26.07	1.39	0.39	2.69	0.75	50.11	0.29
EFB-HCl	2.28	0.94	4.83	1.48	0.19	0.32	1.54	66.46	0.52
PMF-HCl	5.26	0.18	7.32	1.41	0.19	0.18	1.76	65.47	0.12
PKS-$HClO_4$	7.77	0.88	29.95	1.43	0.25	0.47	0.94	47.95	0.38
EFB-$HClO_4$	1.97	0.39	6.92	1.03	0.13	0.14	1.46	63.57	0.19
PMF-$HClO_4$	4.90	0.54	9.16	1.45	0.15	0.15	1.47	62.24	0.16
PKS-H_2SO_4	9.03	6.16	29.81	1.27	0.19	0.37	0.91	40.33	0.22
EFB-H_2SO_4	2.00	0.62	3.70	0.91	0.11	–	1.70	66.23	0.15
PMF-H_2SO_4	5.05	0.40	7.42	1.42	0.15	0.13	1.34	66.79	0.07
PKS-HF	1.67	69.10	3.73	0.18	0.79	0.16	0.23	0.81	0.02
EFB-HF	1.08	42.26	8.41	0.58	5.09	–	4.73	3.45	0.51
PMF-HF	4.88	32.42	10.49	4.19	3.37	0.50	3.54	6.45	0.22
PKS-HNO_3	7.08	5.75	31.30	1.13	0.28	0.57	0.67	46.56	0.20
EFB-HNO_3	2.75	1.14	10.08	1.02	0.20	0.20	1.14	68.82	0.20
PMF-HNO_3	4.73	0.77	8.79	1.12	0.15	0.17	1.27	69.80	0.14

compositional properties of these demineralized biomasses were slightly changed probably due to the removal of a fraction of organic components [19,23,33,34].

Higher heating value (HHV) of the various biomass samples was calculated from the elemental compositions using Eq. (1) and summarized in Table 1. As shown in Table 1, the ash removal was in direct relation with the biomasses HHV increasing.

The XRF results tabulated in Table 2 indicate the major inorganic constituents (Al, Ca, Fe, K, Mg, P and Si) reduction after the biomasses demineralization. The amount of Ca, K, Mg and Si after demineralization showed different degrees of their removal most likely associated with the solubility of the different metal oxides in the various acids. Most of the acid diluted solutions like HCl, H_2SO_4, HNO_3 and $HClO_4$ were very efficient in Ca and Mg reduction, while HF showed considerable results on Si diminution. K_2O and SiO_2 were the main minerals available in EFB and PMF which could be efficiently leached out by HF. CaO, which was the most dominant inorganic species in PKS, efficiently leached out by HCl (from 71.57 to 1.27 wt.%), whereas HF was not successful to remove it. It might be likely attributed to the higher H^+ concentration of HCl compared with HF (weak acid owing to strong H—F bond) due to its higher dissolution in water [23,35]. It is worthwhile to mention that, various diluted acids had different acid strength increasing in the following order: $HClO_4 > HCl > H_2SO_4 > HNO_3 > HF$.

Acid leaching processes are very effective on removal of inorganic species, but it may impose a negative impact on the biomass physiochemical structure. Therefore, investigations on the physiochemical structure of the samples needs to be taken to the consideration.

In this study, among the demineralized biomass samples pretreated by diverse diluted acid solutions, those which showed the maximum inorganics removal have been selected for elaborated analysis. EFB and PMF demineralized by HF and PKS pretreated by HCl indicated maximum ash removal.

3.2. Physical characterization of the biomasses

Fig. 2 shows SEM images of the virgin and pretreated biomass samples with some differences in particle shape. After pretreatment, some morphological changes were observed indicating partial damage in biomasses structure although, their main framework was unchanged. As could be observed in SEM images, there were originally few pores on the surface of untreated biomasses. However, after acid pretreatment, surface porosity of the samples was increased. It was in agreement with the porosity characteristics of the biomasses were shown in Table 3. The virgin biomass samples (Fig. 2a, c, and e) showed small particles adhered to their surfaces. After leaching of EFB (Fig. 2d) and PMF (Fig. 2f) by diluted hydrofluoric acid and pretreatment of PKS by diluted hydrochloric acid (Fig. 2b), some particles were leached away and the biomass samples structure seemed to be eroded. The removed particles from the biomasses samples by various diluted acid solutions might be minerals (Table 2) and extractives [23,36].

All the leached samples showed some changes in the biomasses stomata and epidermis, which could be an evidence for the effects of acid leaching on the fiber structure of biomass samples by dissolving some contents of hemicellulose and probably cellulose [23,37]. On the other hand, partially dissolution of mineral constituents and adhered amorphous hemeicellulose during acid pretreatment resulted higher available surface area and pore volume [38].

Table 3 shows the adsorption characteristics of raw and pretreated biomass samples. All tests were carried out in duplicate to ensure reproducibility of the results; the mean of these two measurements (with less than 3% difference) was taken to represent each evaluation. EFB and PMF leached by HF solution and PKS pretreated by HCl indicated that their total pore volume and BET surface area were both increased, whereas their average pore

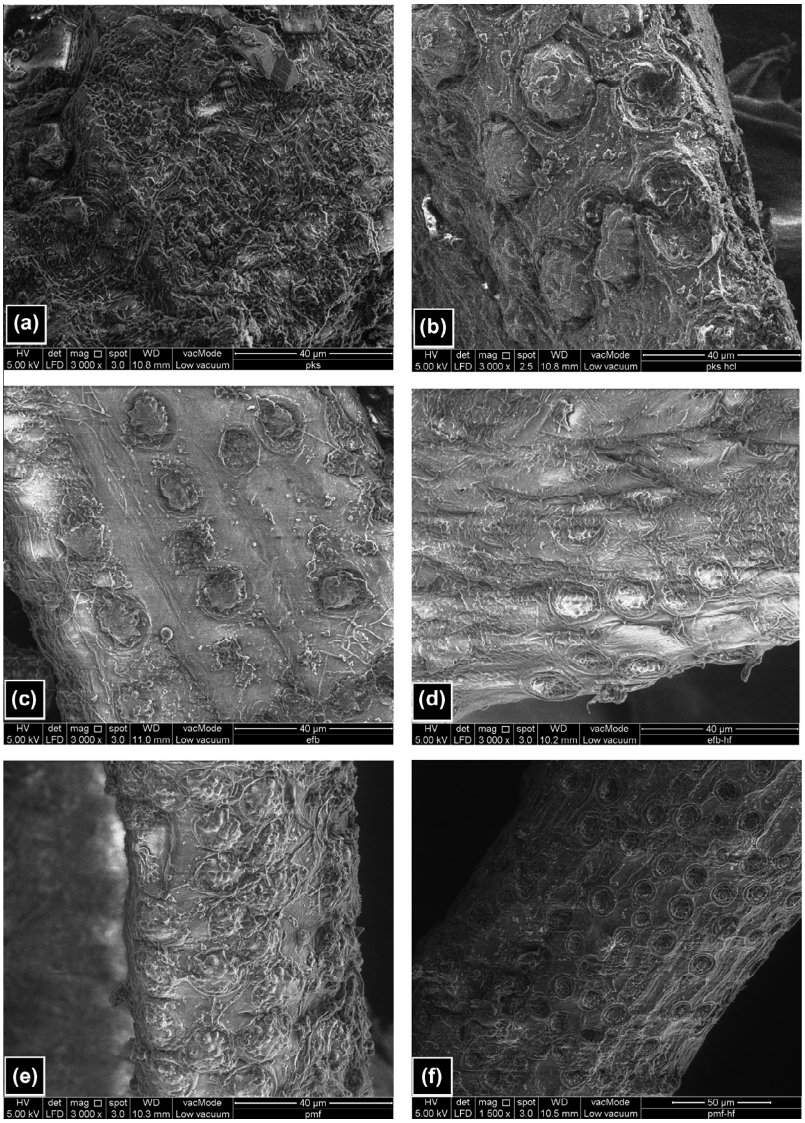

Fig. 2. SEM images of the virgin (PKS (a), EFB (c) and PMF (e)) and pretreated (PKS-HCl (b), EFB-HF (d) and PMF-HF (f)) palm oil biomass samples.

Table 3
Porosity characteristics of the virgin and pretreated biomass samples.

Biomass sample	BET surface area (cm^2/g)	Total pore volume (cm^3/g)	Average pore diameter (nm)
PKS	0.3106	0.001292	45.1133
EFB	0.1188	0.001936	36.0622
PMF	1.2528	0.008705	40.0061
PKS-HCl	0.6051	0.003769	37.3816
EFB-HF	0.9615	0.004993	33.6010
PMF-HF	1.6051	0.009859	29.6556

diameter was decreased. This could indicate that leaching process of the biomass samples by diluted hydrofluoric acid (EFB-HF and PMF-HF) and hydrochloric acid (PKS-HCl) probably eroded the biomass fiber structure and led to the creation of numbers of pores, thus conducted to BET surface and total pore volume increasing. This was in agreement with SEM results explained before.

3.3. Chemical structure evaluation of the biomass samples

The chemical structure of the lignocellulosic biomass samples is frequently studied using infrared spectroscopy. In this investigation, FTIR technique was employed to study the effects of ash removal on the biomasses chemical structure. Fig. 3 depicts the FTIR spectra of the various virgin and pretreated biomasses. Table 4 shows the assignment of FTIR peaks to the chemical functional groups and biomass components according to the literature.

In the infrared spectra, the first strong broad band at 3700–3000 cm^{-1} was related to O—H stretching vibration of phenolic, alcoholic and carboxylic functional groups. Also, the band between 2800 and 3000 cm^{-1} was attributed to C—H stretching vibration of $—CH_2$ and $—CH_3$ functional groups. As can be seen in Fig. 3, both of these bands slightly declined after demineralization, which was in agreement with the studies done by Jiang et al. [23] and Fierro et al. [39].

The band around 1730 cm^{-1} was the result of C=O (aldehydes, ketones or carboxyl) stretching vibration of free carbonyl groups of hemicellulose component. The next spectrum bands around 1650–1510 cm^{-1} (C=C stretching vibrations of aromatics) were corresponded to lignin.

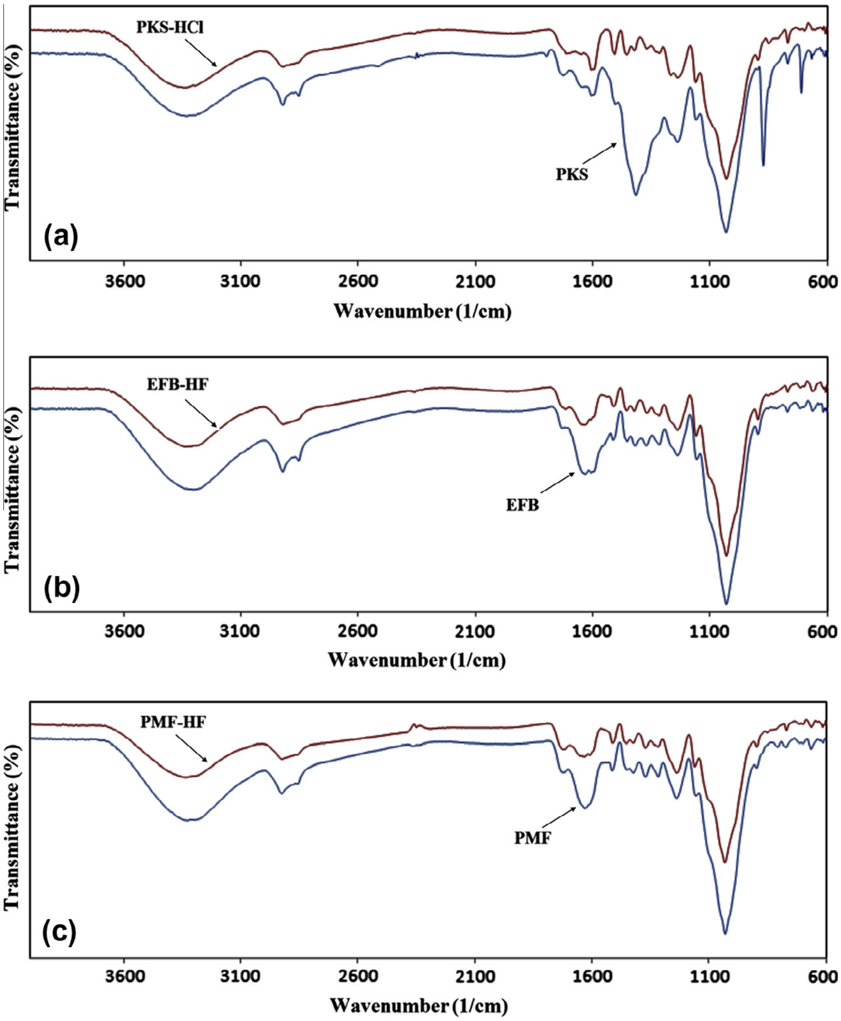

Fig. 3. FTIR spectra of different virgin and pretreated biomass samples. (a) PKS and PKS-HCl; (b) EFB and EFB-HF; (c) PMF and PMF-HF.

Table 4
Assignment of peaks to the chemical functional groups and biomass components using FTIR.

Wavenumbers (cm^{-1})	Vibration	Functional group	Biomass component	Ref.
3700–3000	O—H(Stretch)	Phenolic, alcoholic, carboxylic		[39]
3000–2800	C—H(Stretch)	$—CH_2$, $—CH_3$		[39]
1730	C=O(Stretch)	Carbonyl	Hemicellulose	[42]
1510–1650	C=C(Stretch)	Aromatic ring	Lignin, Cellulose	[39]
1440–1400	O—H(bend)	Alcoholic, carboxylic	Hemicellulose, Cellulose	[43]
1235	COOH(Stretch)	Carbixylic, acetic acid ester	Hemicellulose	[44]
1246–950	C—O—C, C—O, C—OH (Stretch)	Lignin, Polysaccharides	Cellulose, Lignin, Hemicellulose	[42]
850–750	C—H(bend)	Aromatic compounds	Lignin	[40]

After demineralization, slight changes of the intensity of band around 1730 cm^{-1}, compared with more intense change of band around 1650 cm^{-1}, could be attributed to the joint vibration(stretching) of carbonate inorganics and lignin. As indicated in Fig. 3, EFB and PMF showed more significant decrease of the band around 1650 cm^{-1} probably due to the high degree of inorganics (carbonate) removal [23,39].

The spectral region of 1400–600 cm^{-1}, where various vibration modes existed, was very complicated to be analyzed. However, in this region, vibration of some specific units related to lignin could be detected. The spectra of different samples indicated the characteristic vibration of lignin unit at 1240 cm^{-1} (C=O stretching) and 850–750 cm^{-1} (C—H bending) [39,40]. Among different biomass samples, PKS pretreated by HCl showed more considerable changes of these bands intensity compared with EFB-HF and PMF-HF.

The spectra between 1440 and 1400 cm^{-1} contained several bands in the O—H bending region, which were most probably cellulose and hemicellulose related transmission. A significant change of bands intensity in this region could be observed for PKS-HCl (Fig. 3a).

Changing of the spectra (after biomasses pretreatment) at 1730 cm^{-1} and between 950 and 1200 cm^{-1} could be due to C—O—C, C—O and C—OH functional groups stretching, most likely related to hemicelluloses and cellulose components.

As can be seen in Fig. 3, unlike PKS, the virgin EFB and PMF indicated relatively similar chemical structure. Also, after pretreatment they exhibited rather comparable FTIR spectra. It might be attributed to the leaching acids type and the biomasses nature and composition already explained in Section 3.1. Pretreatment of EFB and PMF by diluted hydrofluoric acid introduced slight effects on the biomasses chemical structure [19,41], whereas leached PKS by hydrochloric acid showed more considerable changes in the biomass chemical structure.

3.4. Pyrolysis characteristics

Fig. 4 shows the TGA (weight loss) and DTG (derivative thermogravimetric) analysis evolution profiles as a function of temperature for the virgin and pretreated palm oil biomass samples at a constant heating rate of 15 °C/min. As a whole, the pyrolysis process of the lignocellulosic biomass can be divided into four main sections: moisture and very light volatiles components removal (<120 °C); degradation of hemicellulose (220–315 °C); lignin and cellulose decomposition (315–400 °C) and lignin degradation (>450 °C) [11,43]. As indicated in Fig. 4, various untreated (virgin) palm oil biomass samples showed different thermal behavior. The DTG peaks attributed to cellulose decomposition were observed at 364 °C, 329 °C and 351 °C for PKS, EFB and PMF, respectively. The DTG shoulders of PKS and PMF curves observed at ~300 °C were caused by hemicelluloses devolatilisation [45,46]. The palm oil biomasses lignin decomposition was occurred slowly over a broad range of temperature (137–667 °C) [46]. In the section corresponded to lignin degradation (>450 °C), EFB overlapped PMF, whereas that of PKS occurred with different weight loss rates indicating one peak in DTG curve started at about 650 °C.

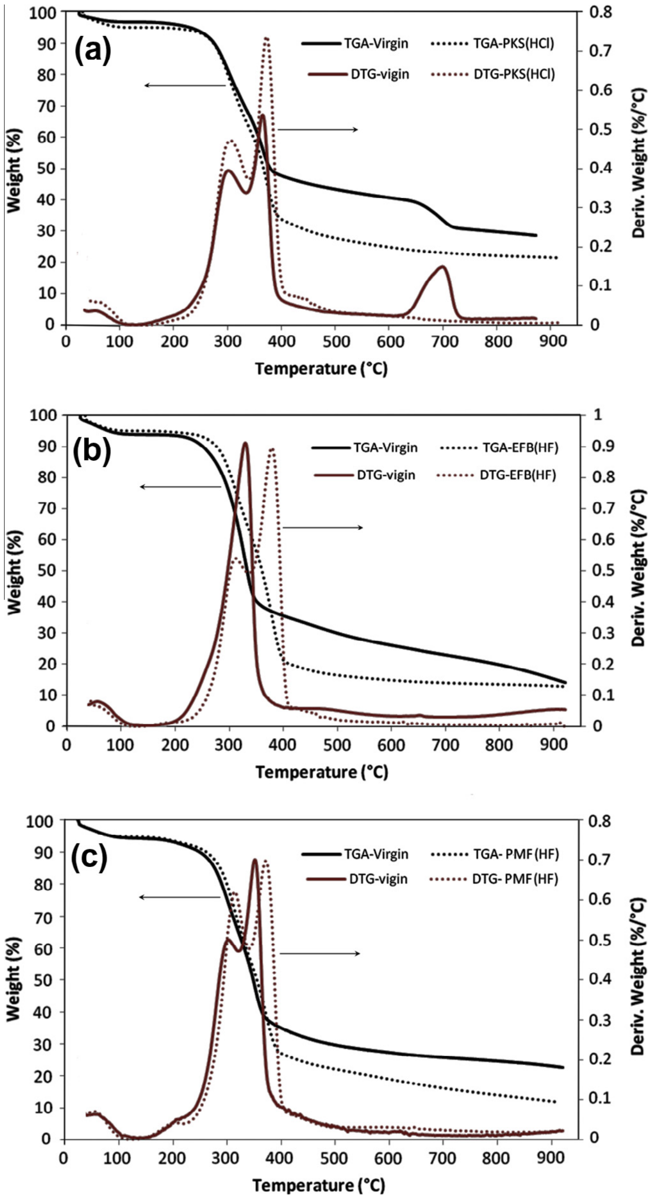

Fig. 4. Thermogravimetric analysis (TGA) and differential thermogravimetic (DTG) curves of the virgin and demineralized palm oil biomass samples during pyrolysis process. (a) PKS and PKS-HCl; (b) EFB and EFB-HF; (c) PMF and PMF-HF; N_2 gas flow rate: 150 ml/min; Heating rate: 15 °C/min.

The different thermal behavior of the lignocellulosic materials could be attributed to the various contents of cellulose, hemicellulose and lignin (Section 3.1) [10,11]. The lowest temperature peak in DTG curve could indicate the highest content of hemicellulose in EFB. Furthermore, the differences in residue yield could represent the different lignin contents of the biomass samples. PKS indicated the highest content of the lignin due to the largest residue. Also, maximum weight loss rate could be an indication of volatile matters and cellulose content in the biomass samples [47]. The maximum decomposition rate of EFB was higher than that of PKS and PMF, because its cellulose and volatiles contents were greater.

DTG curve corresponded to PKS showed a third isolated peak started at temperature ~650 °C and reached to maximum at ~700 °C. Literature investigations on similar sample indicated that except Idris et al [45], who reported this third peak, it has not been expressed elsewhere. Further details on the reasons for occurrence of this peak would be explained in Section 3.6 using TGA-MS and TGA-FTIR analysis.

Reactivity of the biomass samples can be estimated from the peak height and position. The peak height is directly proportional to the biomass reactivity, whereas the temperature in which the peak takes place is inversely proportional to the biomass reactivity [46]. As can be seen in Fig. 4b, the highest degradation rate belonged to EFB at lowest peak temperature. So, EFB indicated the highest reactivity among palm oil biomass samples [45].

As shown in Fig. 4, regardless of the biomass sample type and pretreatment process, all the biomass samples were pyrolyzed at the temperature range of ~250 °C to ~400 °C.

From literature it is known that hemicellulose is degraded at peak temperature of ~300 °C, while cellulose is decomposed at the peak ~365 °C [10,11,25,26]. As can be observed in Fig. 4b, demineralized EFB by diluted HF solution showed a shoulder in the relevant peak at around 311 °C in DTG curve. It was caused by hemicellulose decomposition, while the peak at 379 °C was associated with cellulose degradation. However, cellulose and hemicellulose decomposition in the virgin EFB biomass were overlapped due to the presence of inorganics. In this case, the catalytic effects of inorganics moved cellulose pyrolysis to lower temperature and combined together with the pyrolysis of hemicellulose.

DTG curves related to PMF and PMF-HF have been shown in Fig. 4c. As represented in Fig. 4c, peak shoulder showed hemicellulose decomposition, while the main peak indicated cellulose degradation. Deminiralization shifted hemicellulose and cellulose degradation to a higher temperature (351 °C and 371 °C, respectively). The same could be observed for PKS and PKS-HCl (Fig. 4a). Unlike EFB and PMF, PKS showed third peak at ~700 °C. This peak was disappeared whilst PKS demineralized by HCl solution. It was possibly due to the catalytic effects of minerals at high temperature (~650 °C ~750 °C). An elaborated study on this phenomenon would be expressed in Section 3.6.

As explained in Section 3.1, K_2O and SiO_2 (the main minerals available in EFB and PMF) could be efficiently leached out by HF, whereas CaO (which was the most dominant inorganic species in PKS) could be highly extracted by HCl. Since their elimination changed the biomass thermal behavior, they probably had significant effects on the catalytic behavior of inorganics available in the various biomasses.

Pretreatment has a significant influence on the biomasses thermal behavior in terms of both gas product distributions and pyrolysis temperature. Considering DTG curves in Fig. 4, pretreatment using the diluted acid solutions transferred the biomass samples pyrolysis to a higher temperature by 5–50 °C. Pyrolysis properties of the virgin and pretreated palm oil biomass samples using TGA and DTG are summarized in Table 5. As reported in Table 5, in comparison with the virgin samples, the maximum decomposition rate of HF pretreated biomass samples around 365 °C (cellulose components degradation) was almost unchanged, whereas HCl pretreated samples showed considerable increase in degradation rate from 0.535%/°C to 0.737%/°C. These changes in cellulose components decomposition rate was associated with cellulose crystallinity and structure. Therefore, it could be concluded that the biomass pretreatment by HCl relatively disrupted cellulose crystalline, whereas HF had not significant effect on cellulose structure. These results are similar to those reported by Eom et al. [19]. The lignocellulosic biomass pretreatment with HF solution could be interesting from two main aspects; (a) its efficient demineralization effects on the reduction of biomass samples (here EFB and PMF) ash content to negligible amount [19,41] and (b) unlike most of the acids pretreatments which considerably changed the biomass chemical structure (degradation) during pretreatment, HF did not indicate significant effects on the biomass chemical degradation during the demineralization. Therefore, more precise effects of demineralization on the biomass samples thermal behavior could be investigated [19].

Moreover, as can be seen in Table 5, the char yield decreased after deashing pretreatment. This indirectly could be an evidence for the effect of the biomass demineralization on the production of more volatile components during pyrolysis.

The first peak in the various DTG curves in Fig. 4 indicated the moisture content of the biomass samples dropped rapidly at the temperature of ~60 °C (Table 3). This observation was thanks to the significant moisture evaporation as temperature increased.

3.5. Kinetics analysis results

Referring to Eq. (7) and applying the TGA (mass change by temperature) results, $\ln[-\ln(1-x)/T^2]$ versus $1/T$ was plotted for the virgin and pretreated biomass samples. Among TGA data, those which provided the best linear regression were selected. Therefore, from the calculated slope and intercept ($-E_a/R$ and $\ln[k_0R/\beta E_a]$, respectively), the kinetics parameters (pre-exponential factor (k_0) and activation energy (E_a)) were determined. The results of kinetics parameters at corresponded temperature are shown in Table 6. Calculated regression results having coefficient of determination (R^2) from 0.9930 to 0.9990 and standard error from 7.83×10^{-7} to 6.19×10^{-6} indicated that the assumption of the biomass pyrolysis reaction undergoing a first order reaction should be proper. High R^2 coefficient and low standard error values could prevent the data noise (experimental errors disturbance) and provide more reliable kinetic parameters at related temperature ranges.

As can be seen in Table 6, activation energy varied after biomasses demineralization. Compared with the virgin biomasses

Table 5
Pyrolysis properties of the virgin and demineralized palm oil biomass samples using TGA and DTG; N_2 gas flow rate: 150 ml/min; Heating rate: 15 °C/min.

Biomass	Maximum temperature (°C)				Maximum Deriv. Weight (wt.%/°C)				Char Content (wt.%)
	First peak	Shoulder	Second peak	Third peak	First Peak	Shoulder	Second Peak	Third Peak	
PKS	61	300	364	700	0.035	0.395	0.535	0.148	29.3
PKS-HCl	62	305	373	–	0.059	0.47	0.737	–	22.2
EFB	60	–	329	–	0.078	–	0.90	–	14.5
EFB-HF	61	311	379	–	0.061	0.54	0.895	–	13.0
PMF	61	301	351	–	0.064	0.50	0.70	–	22.2
PMF-HF	60	314	371	–	0.070	0.62	0.70	–	13.0

Table 6
The pyrolysis kinetics parameters of the biomass samples.

Biomass	Temperature range (°C)	K_0 (1/s)	E_a (kJ/mol)	R^2	Standard error
PKS	250–270	8.7×10^{-1}	34.10	0.9944	3.72×10^{-6}
	280–320	2.50×10^{2}	57.28	0.9960	3.54×10^{-6}
PKS-HCl	260–280	1.07×10^{1}	44.37	0.9931	1.97×10^{-6}
	280–320	1.24×10^{3}	64.52	0.9974	1.79×10^{-6}
EFB	250–270	1.00×10^{0}	33.81	0.9986	7.83×10^{-7}
	280–320	6.00×10^{2}	60.30	0.9957	2.32×10^{-6}
EFB-HF	260–280	1.05×10^{0}	35.64	0.9960	1.89×10^{-6}
	280–320	2.31×10^{3}	68.10	0.9990	1.11×10^{-6}
PMF	250–270	1.60×10^{-1}	26.11	0.9970	2.06×10^{-6}
	275–360	1.15×10^{2}	52.66	0.9976	3.46×10^{-6}
PMF-HF	260–280	2.23×10^{-1}	28.64	0.9932	1.85×10^{-6}
	275–360	1.63×10^{2}	55.78	0.9930	6.19×10^{-6}
Bamboo leaves [10]	195–220	2.10×10^{-1}	31.41	0.9980	
	245–280	5.85×10^{2}	62.74	0.9996	
Sugarcane peel [10]	180–205	2.76×10^{1}	50.03	0.9990	
	250–290	2.42×10^{2}	59.27	0.9998	

(26.11–60.30 kJ/mol), the acid pretreated samples showed higher activation energy varied in the range of 28.64–68.10 kJ/mol associated with minerals removal. The catalytic effects of various inorganic constituents available in the biomasses altered their thermal behavior. It is worthwhile to know that, the biomass inorganic composition has also significant effect on its catalytic performance [41]. At pyrolysis temperatures of 280–320 °C, the moderate reactivity of PKS, EFB, PMF and their pretreated samples could be an indication of multi-components composite reactions. It means, part of the three main biomass building blocks comprising cellulose, hemicellulose and lignin were decomposed at this temperature range. The pre-exponential factor (k_0) for the virgin biomass samples at the temperature range of 280–320 °C were 1.15×10^2–6.00×10^2 1/s, while pretreated samples showed 1.63×10^2–2.31×10^3 1/s. The pyrolysis kinetics data calculated by the present investigation were in agreement with the similar kinetics studies earlier reported assuming first-order lignocellulosic biomass pyrolysis reaction [10,15,46]. Various virgin biomass samples indicated different pyrolysis kinetics parameters (activation energy and pre-exponential factor). These parameters were highly influenced by the composition and type of biomass feedstock [11]. The calculated biomasses activation energy and pre-exponential factors did not differ much from the kinetic parameters of bamboo leaves and sugarcane peel biomasses investigated in the literature assuming first order reaction kinetics.

The activation energy and pre-exponential factors shown in Table 6 indicated an increasing tendency with the temperature rising. The kinetics parameters exhibited a kinetic compensation effect, which could be sort of interdependence between them. There were positive correlation between the activation energy and pre-exponential factor. The latest might be due to the fact that the pre-exponential factor was greatly related with the temperature dependent collision frequency explained in collision theory. Some components of the biomass like hemicelluloses could be pyrolyzed at lower temperature. Lower activation energy at lower temperature was possibly attributed to the decomposition of the mentioned biomass components.

As explained, in this kinetics studies, some part of TGA data which could provide the best linear regression results were selected. Therefore, pre-exponential factor (k_0) and activation energy (E_a) were calculated from straight line intercept and slope, respectively. Since the thermal behavior of the lignocellulosic biomass may vary during the pyrolysis due to their complex composition, therefore too many poor regression data may be resulted. So, in this investigation, TGA data over narrow ranges of temperature could provide a good linear regression.

3.6. Evolved gas analysis

3.6.1. TGA-MS analysis of gas products

TGA-MS technique can identify and analyze simultaneously the evolved gas during the biomass pyrolysis in real time. The primary pyrolysis products are mainly condensable gases and solid char. The condensable gases might be further decomposed through gas phase homogenous and gas–solid heterogeneous reactions into noncondensable gases, liquid and char [48]. To study the effects of the biomass samples demineralization on the gaseous products evolution during pyrolysis, the present investigation focused on the production of noncondensable permanent gases like CO_2, CO and H_2 having the atomic mass units (a.m.u) 44, 28 and 2, respectively [28] across the temperature range of 35–850 °C. Fig. 5 shows the mass spectroscopy (MS) spectra for the virgin and pretreated biomass samples. As indicated in Fig. 5, most of the aforementioned gases were produced at the temperature range of 250–750 °C probably attributed to the biomasses oxygenated functional groups cleavage, inorganic species decomposition and some secondary reactions like steam reforming (Eq. (8)), water–gas shift reaction (Eq. (9)) and char gasification with water (Eqs. (10) and (11)) [11,49]. As can be seen in Fig. 5, the production of CO_2, CO and H_2 gases were in strong correlation with the biomass reactivity. Inorganic constituents, which probably catalyzed the pyrolysis reactions, increased the biomass reactivity. The acid pretreated palm oil biomass samples showed lower gas evolution compared with the virgin samples. CO_2 and CO evolutions during pyrolysis might be attributed to the cleavage of oxygen containing functional groups via decarboxylation and decarbonylation reactions, respectively. Decreasing in CO_2 and CO release after biomasses demineralization could demonstrate the catalytic role of inorganic species.

At high temperature (above 600 °C), the coincident occurrence of CO_2, CO and H_2 peaks for the virgin PKS could be an evidence for char decomposition through water–gas shift reaction. High content of CaO (71.6 wt.% according to XRF results) in the virgin PKS could catalyze this type of reaction. Also, some fraction of CO_2, CO generation at this temperature might be due to inorganic carbonates degradation. Disappearance of these peaks after PKS acid pretreatment (minerals elimination) could be a reasonable evidence for the catalytic effects of inorganics.

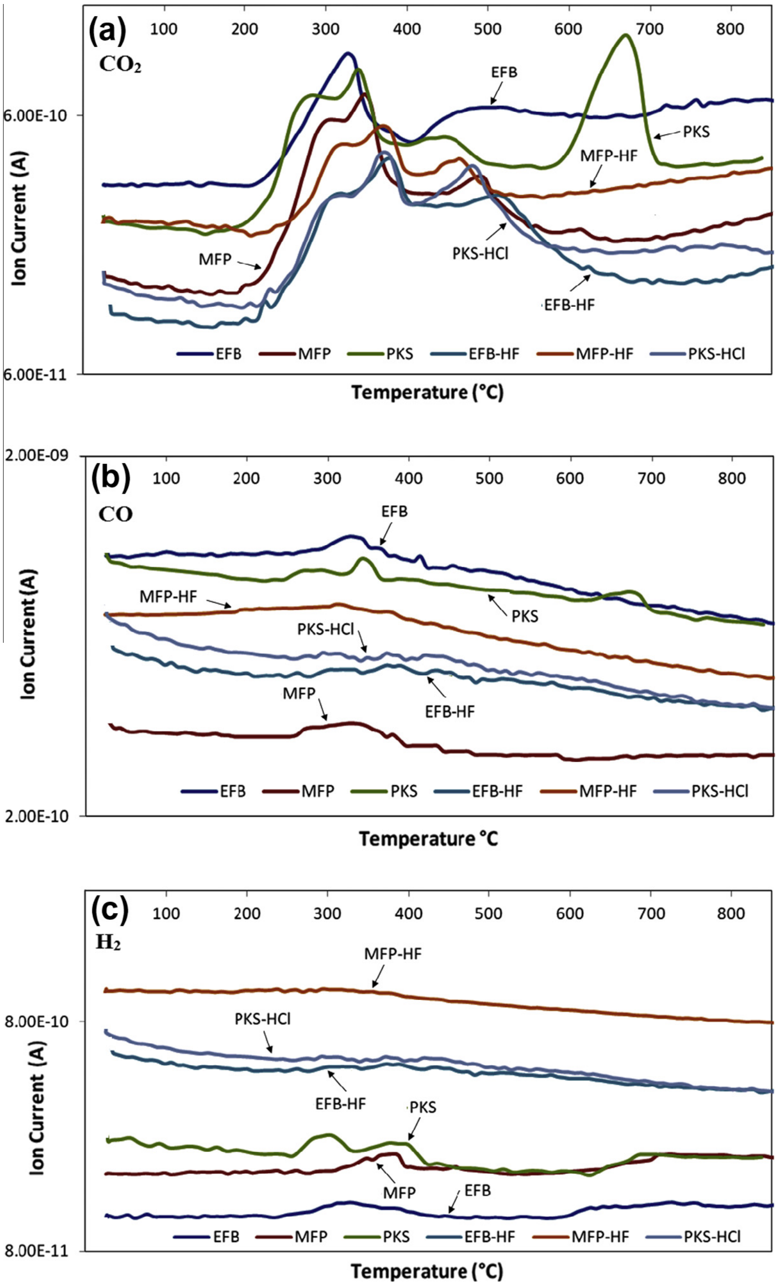

Fig. 5. Mass spectra (MS) related to the gas products from pyrolysis of the different virgin and pretreated palm oil biomass samples: (a) CO_2, (b) CO and (c) H_2 detection.

$$CH_4 + H_2O \leftrightarrow CO + 3H_2 \text{ (Steam reforming)} \tag{8}$$

$$C + H_2O \leftrightarrow CO_2 + H_2 \text{ (Water-gas shift)} \tag{9}$$

$$C + H_2O \leftrightarrow CO + H_2 \text{ (Char gasification)} \tag{10}$$

$$C + 2H_2O \leftrightarrow CO_2 + 2H_2 \text{ (Char gasification)} \tag{11}$$

H_2 formation from the virgin palm oil biomass samples at temperature above 600 °C (where CO and CO_2 evolution were not observed) could be probably caused by hydrocarbons (aromatics and aliphatics) thermal cracking and dehydrogenation (Eq. (12)) [50]. These reactions most likely were catalyzed by the mineral constituents presented in the biomass samples. As indicated in Fig. 5c, after the biomasses demineralization, a significant decrease in H_2 evolution was observed.

$$C_nH_m \leftrightarrow C_{n-x}H_{m-y} + H_2 + C + CH_4 \quad \text{(thermal cracking)} \tag{12}$$

The studies on the effects of inorganics on the biomasses thermal behavior indicated that their presence increased permanent gas yield during pyrolysis and lowered the pyrolysis temperature.

The investigations on the thermogravimetric analysis and evolved gas data presented some information about the biomass samples reactions. In the temperature range ~250 °C < T < ~400 °C, where pyrolysis reactions (most part of cellulose and hemicellulose degradation) was occurred, the significant amount of gases were released. Demineralization shifted the maximum pyrolysis (Fig. 4) and gas evolution (Fig. 5) to a higher temperature. For the biomass samples, in the temperature range ~400 °C < T < ~600 °C, CO_2 generation was observed, whereas CO was not detected. It probably could indicate the existence a pathway of secondary reactions which diminished the CO evolution (Eq. (13)).

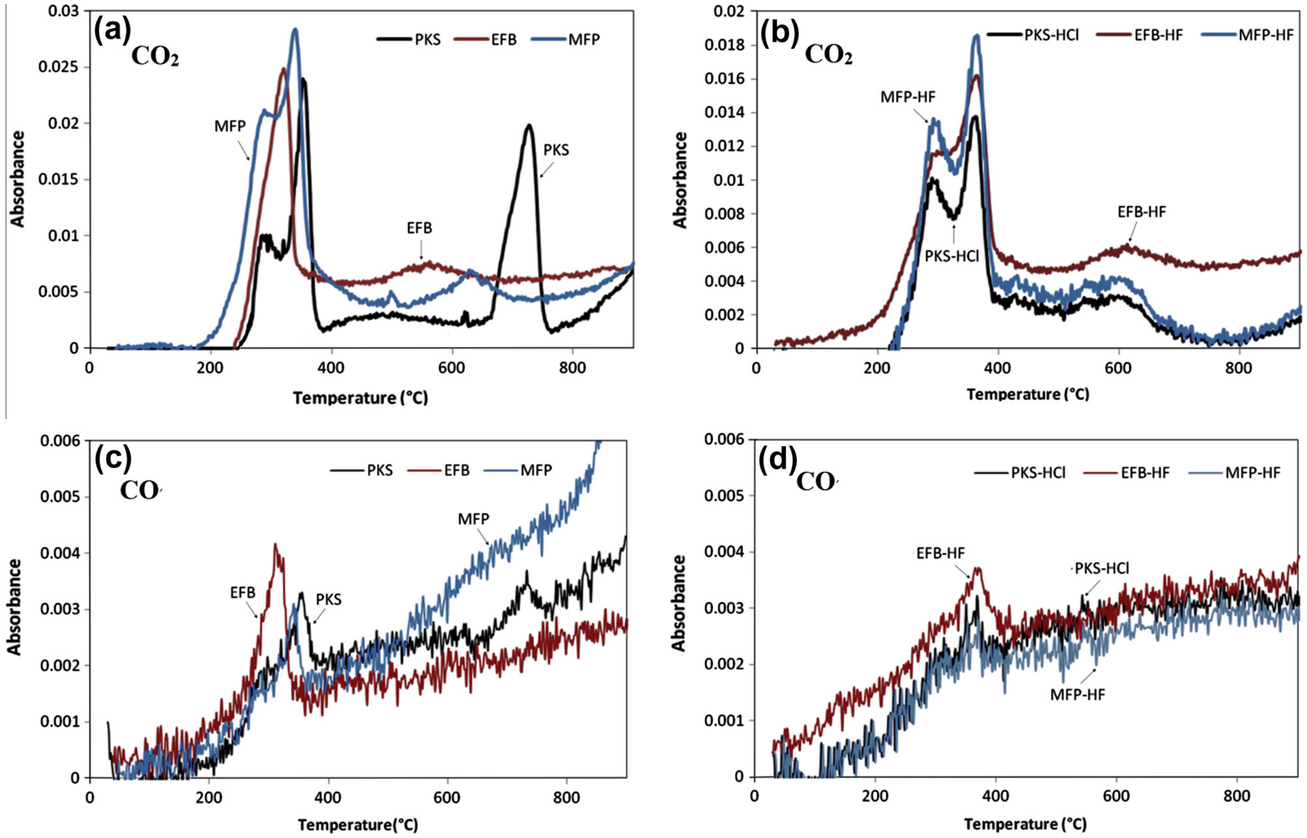

Fig. 6. FTIR spectra of the permanent released gas during the palm oil biomass samples pyrolysis: (a) CO_2 detection from the virgin biomasses. (b) CO_2 detection from the pretreated biomasses. (c) CO detection from the virgin biomasses. (d) CO detection from the pretreated biomasses.

$$CO + 0.5O_2 \leftrightarrow CO_2 \tag{13}$$

where O_2 could be originated from the condensable gases further degradation and inorganic carbonates decomposition.

3.6.2. TGA-FTIR analysis of gas products

The produced pyrolysis vapors from the biomass samples were analyzed by using the FTIR spectroscopy to study the effects of the biomass demineralization on the permanent gases production. Going deeper to the issue and to verify the TGA-MS results earlier explained, TGA-FTIR was employed to analyze the CO_2 and CO gases evolution in the temperature range 35–850 °C. The released gases were measured online using TGA coupled with FTIR. The formation of CO_2 at 2402–2240 cm^{-1} could be attributed to the cracking and reforming of the organics functional groups like carbonyl (C═O) and carboxyl (—C (═O) O—). Also, it may be caused by inorganic carbonates decomposition [9,51,52]. Further, the characteristic peaks of CO, which could be attributed to C═O and —C (═O) O— functional groups breakage, were observed at the bands 2240–2000 cm^{-1}[9,53]. As explained before, CO_2 and CO formation may be also attributed to the secondary degradation of char and volatile components [9,51].

Fig. 6 depicts the FTIR spectrums of CO_2 and CO release during the biomasses (virgin and demineralized) pyrolysis. The major CO_2 evolution for the virgin palm oil biomass samples was detected in the temperature range ~250 to ~350 °C, while demineralized samples showed its major detection shifted to higher temperature range (~290 to ~370 °C). This phenomenon could confirm the catalytic role of inorganic constituents, which is in direct relation with the biomasses reactivity, during thermal analysis. It is in agreement with the TGA-MS results explained before.

As indicated in Fig. 6a and b, PKS showed a peak at temperature about ~700 °C for CO_2 release. This peak was disappeared after PKS demineralization by HCl. This phenomenon could be an evidence of catalytic effect of inorganics on CO_2 formation at temperature ~700 °C.

Considering CO evolution, as shown in Fig. 6c and d, most of the released gases from the virgin biomasses were detected in temperature range ~300 °C to ~360 °C, while the demineralized biomass samples showed very low intensity absorption peak at 350–400 °C. Virgin PKS illustrated a CO peak at about 700 °C, whereas this peak was not observed after demineralization by HCl. This could also confirm the catalytic behavior of minerals available in the biomasses at about ~700 °C. On the other hand, CO_2 and CO peaks for the virgin PKS at high temperature (>600 °C) could be also attributed to the char and inorganic carbonates degradation reactions.

4. Conclusion

The different palm oil biomass samples (PKS, EFB and PMF) were demineralized by diverse diluted acid solutions (H_2SO_4, $HClO_4$, HF, HNO_3, HCl). HF pretreatment showed interesting results on significant minerals removal from EFB and PMF, whereas HCl indicated considerable inorganic constituent removal from PKS. The pretreated biomasses, which exhibited the highest efficiency of minerals removal, were deeply investigated. Their physiochemical structure studies showed that acid pretreatment introduced some impacts on the structure of the biomass samples. The virgin and demineralized biomasses thermal behavior and evolved gases (H_2, CO_2 and CO) produced during pyrolysis were investigated by TGA-MS and TGA-FTIR. Most of these gaseous products were generated at pyrolysis temperature between 250 and 400 °C, while at high temperature (>600 °C) the dominant released gas was hydrogen. The kinetics model satisfactorily predicted the biomasses pyrolysis behavior. The shift of pyrolysis to higher temperature, diminishing of the released gas and activation energy enhancement after demineralization could suggest the catalytic effects of the biomasses inorganics.

The outcome of the present analysis investigation provides valuable information can be employed for the efficient thermochemical conversion of the palm oil biomasses.

Acknowledgments

The authors would like to acknowledge the financial support from the High Impact Research (HIR) Grant (UM.C/625/1/HIR/MOHE/ENG/11 from the Ministry of Higher Education Malaysia), Chemical Engineering Department, Faculty of Engineering, University of Malaya, Malaysia.

References

[1] Bridgwater AV, Meier D, Radlein D. An overview of fast pyrolysis of biomass. Org Geochem 1999;30:1479.

[2] Zhang L, Xu C, Champagne P. Overview of recent advances in thermo-chemical conversion of biomass. Energy Convers Manage 2010;51:969–82.

[3] Wilson L, Yang W, Blasiak W, John GR, Mhilu CF. Thermal characterization of tropical biomass feedstocks. Energy Convers Manage 2011;52:191–8.

[4] Çepelioğullar Ö, Pütün AE. Thermal and kinetic behaviors of biomass and plastic wastes in co-pyrolysis. Energy Convers Manage 2013;75:263–70.

[5] Fernandes ERK, Marangoni C, Souza O, Sellin N. Thermochemical characterization of banana leaves as a potential energy source. Energy Convers Manage 2013;75:603–8.

[6] Magdziarz A, Wilk M. Thermogravimetric study of biomass, sewage sludge and coal combustion. Energy Convers Manage 2013;75:425–30.

[7] Chen D, Zheng Y, Zhu X. In-depth investigation on the pyrolysis kinetics of raw biomass. Part I: Kinetic analysis for the drying and devolatilization stages. Bioresour Technol 2013;131:40–6.

[8] White JE, Catallo WJ, Legendre BL. Biomass pyrolysis kinetics: a comparative critical review with relevant agricultural residue case studies. J Anal Appl Pyrol 2011;91:1–33.

[9] Edreis EMA, Luo G, Li A, Chao C, Hu H, Zhang S, et al. CO_2 Co-gasification of lower Sulphur Petroleum coke and Sugar Cane Bagasse via TG-FTIR Analysis Technique. Bioresource Technol; 2013.

[10] Huang YF, Kuan WH, Chiueh PT, Lo SL. Pyrolysis of biomass by thermal analysis-mass spectrometry (TA-MS). Bioresour Technol 2011;102:3527–34.

[11] Sanchez-Silva L, Lopez-Gonzalez D, Villasenor J, Sanchez P, Valverde JL. Thermogravimetric-mass spectrometric analysis of lignocellulosic and marine biomass pyrolysis. Bioresour Technol 2012;109:163–72.

[12] Otero M, Sanchez ME, Gomez X. Co-firing of coal and manure biomass: a TG-MS approach. Bioresour Technol 2011;102:8304–9.

[13] Basta AH, Fierro V, Saied H, Celzard A. Effect of deashing rice straws on their derived activated carbons produced by phosphoric acid activation. Biomass Bioenergy 2011;35:1954–9.

[14] Eom IY, Kim JY, Kim TS, Lee SM, Choi D, Choi IG, et al. Effect of essential inorganic metals on primary thermal degradation of lignocellulosic biomass. Bioresour Technol 2012;104:687–94.

[15] Yang H, Yan R, Chen H, Zheng C, Lee D, Liang D. Influence of mineral matter on pyrolysis of palm oil wastes. Combust Flame 2006;146:605–11.

[16] Das P, Ganesh A, Wangikar P. Influence of pretreatment for deashing of sugarcane bagasse on pyrolysis products. Biomass Bioenergy 2004;27:445–57.

[17] Liu X, Bi XT. Removal of inorganic constituents from pine barks and switchgrass. Fuel Process Technol 2011;92:1273–9.

[18] Fahmi R, Bridgwater AV, Darvell LI, Jones JM, Yates N, Thain S, et al. The effect of alkali metals on combustion and pyrolysis of Lolium and Festuca grasses, switchgrass and willow. Fuel 2007;86:1560–9.

[19] Eom IY, Kim KH, Kim JY, Lee SM, Yeo HM, Choi IG, et al. Characterization of primary thermal degradation features of lignocellulosic biomass after removal of inorganic metals by diverse solvents. Bioresour Technol 2011;102:3437–44.

[20] Carrier M, Neomagus HW, Grgens J, Knoetze JH. Influence of chemical pretreatment on the internal structure and reactivity of pyrolysis chars produced from sugar cane bagasse. Energy Fuels 2012;26:4497–506.

[21] Fahmi R, Bridgwater AV, Donnison I, Yates N, Jones JM. The effect of lignin and inorganic species in biomass on pyrolysis oil yields, quality and stability. Fuel 2008;87:1230–40.

[22] Álvarez P, Santamaría R, Blanco C, Granda M. Thermal degradation of lignocellulosic materials treated with several acids. J Anal Appl Pyrol 2005;74:337–43.

[23] Jiang L, Hu S, Sun LS, Su S, Xu K, He LM, et al. Influence of different demineralization treatments on physicochemical structure and thermal degradation of biomass. Bioresour Technol 2013;146:254–60.

[24] Ruan R, Yang C, Zhang B, Lin X, Chen L, Wan Y. Improved process for preparing bio-oils from biomass. Google Patents; 2010.

[25] Müller-Hagedorn M, Bockhorn H, Krebs L, Müller U. A comparative kinetic study on the pyrolysis of three different wood species. J Anal Appl Pyrol 2003;68–69:231–49.

[26] Nowakowski D, Jones J, Brydson R, Ross A. Potassium catalysis in the pyrolysis behaviour of short rotation willow coppice. Fuel 2007;86:2389–402.

[27] Channiwala SA, Parikh PP. A unified correlation for estimating HHV of solid, liquid and gaseous fuels. Fuel 2002;81:1051–63.

[28] Huang YF, Chiueh PT, Kuan WH, Lo SL. Pyrolysis kinetics of biomass from product information. Appl Energy 2013;110:1–8.

[29] Huang YF, Kuan WH, Chiueh PT, Lo SL. A sequential method to analyze the kinetics of biomass pyrolysis. Bioresour Technol 2011;102:9241–6.

[30] Coats AW, Redfern JP. Kinetic parameters from thermogravimetric data. Nature 1964;201.

[31] Lu K-M, Lee W-J, Chen W-H, Lin T-C. Thermogravimetric analysis and kinetics of co-pyrolysis of raw/torrefied wood and coal blends. Appl Energy 2013;105:57–65.

[32] Mohammed MAA, Salmiaton A, Wan Azlina WAKG, Mohammad Amran MS, Fakhru'l-Razi A, Taufiq-Yap YH. Hydrogen rich gas from oil palm biomass as a potential source of renewable energy in Malaysia. Renew Sustain Energy Rev 2011;15:1258–70.

[33] Lim WS, Kim JY, Kim HY, Choi JW, Choi IG, Lee JW. Structural properties of pretreated biomass from different acid pretreatments and their effects on simultaneous saccharification and ethanol fermentation. Bioresour Technol 2013;139:214–9.

[34] Eom IY, Kim JY, Lee SM, Cho TS, Yeo H, Choi JW. Comparison of pyrolytic products produced from inorganic-rich and demineralized rice straw (Oryza sativa L.) by fluidized bed pyrolyzer for future biorefinery approach. Bioresour Technol 2013;128:664–72.

[35] Habbache N, Alane N, Djerad S, Tifouti L. Leaching of copper oxide with different acid solutions. Chem Eng J 2009;152:503–8.

[36] Haykiri-Acma H, Yaman S, Kucukbayrak S. Burning characteristics of chemically isolated biomass ingredients. Energy Convers Manage 2011;52:746–51.

[37] Vassilev SV, Baxter D, Andersen LK, Vassileva CG, Morgan TJ. An overview of the organic and inorganic phase composition of biomass. Fuel 2012;94:1–33.

[38] Yu CT, Chen WH, Men LC, Hwang WS. Microscopic structure features changes of rice straw treated by boiled acid solution. Ind Crops Prod 2009;29:308–15.

[39] Fierro V, Torne-Fernandez V, Celzard A, Montane D. Influence of the demineralisation on the chemical activation of Kraft lignin with orthophosphoric acid. J Hazard Mater 2007;149:126–33.

[40] Parshetti GK, Kent Hoekman S, Balasubramanian R. Chemical, structural and combustion characteristics of carbonaceous products obtained by hydrothermal carbonization of palm empty fruit bunches. Bioresource Technol 2013;135:683–9.

[41] Eom I-Y, Kim J-Y, Lee S-M, Cho T-S, Choi I-G, Choi J-W. Study on the thermal decomposition features and kinetics of demineralized and inorganic metal-impregnated lignocellulosic biomass. J Ind Eng Chem 2012;18:2069–75.

[42] Mayer ZA, Apfelbacher A, Hornung A. Effect of sample preparation on the thermal degradation of metal-added biomass. J Anal Appl Pyrol 2012;94:170–6.

[43] Yang H, Yan R, Chen H, Lee DH, Zheng C. Characteristics of hemicellulose, cellulose and lignin pyrolysis. Fuel 2007;86:1781–8.

[44] Smidt E, Schwanninger M. Characterization of waste materials using FTIR spectroscopy: process monitoring and quality assessment. Spectrosc Lett 2005;38:247–70.

[45] Idris SS, Abd Rahman N, Ismail K, Alias AB, Abd Rashid Z, Aris MJ. Investigation on thermochemical behaviour of low rank Malaysian coal, oil palm biomass and their blends during pyrolysis via thermogravimetric analysis (TGA). Bioresource Technol 2010;101:4584–92.

[46] Vamvuka D, Kakaras E, Kastanaki E, Grammelis P. Pyrolysis characteristics and kinetics of biomass residuals mixtures with lignite. Fuel 2003;82:1949–60.

[47] Damartzis T, Vamvuka D, Sfakiotakis S, Zabaniotou A. Thermal degradation studies and kinetic modeling of cardoon (Cynara cardunculus) pyrolysis using thermogravimetric analysis (TGA). Bioresour Technol 2011;102:6230–8.

[48] Dong C-Q, Zhang Z-F, Lu Q, Yang Y-P. Characteristics and mechanism study of analytical fast pyrolysis of poplar wood. Energy Convers Manage 2012;57:49–59.

[49] Widyawati M, Church TL, Florin NH, Harris AT. Hydrogen synthesis from biomass pyrolysis with in situ carbon dioxide capture using calcium oxide. Int J Hydrogen Energy 2011;36:4800–13.

[50] Faix O, Jakab E, Till F, Székely T. Study on low mass thermal degradation products of milled wood lignins by thermogravimetry-mass-spectrometry. Wood Sci Technol 1988;22:323–34.

[51] Fu P, Yi W, Bai X, Li Z, Hu S, Xiang J. Effect of temperature on gas composition and char structural features of pyrolyzed agricultural residues. Bioresour Technol 2011;102:8211–9.

[52] Yan J, Jiang X, Han X, Liu J. A TG-FTIR investigation to the catalytic effect of mineral matrix in oil shale on the pyrolysis and combustion of kerogen. Fuel 2013;104:307–17.

[53] Fu P, Hu S, Xiang J, Li P, Huang D, Jiang L, et al. FTIR study of pyrolysis products evolving from typical agricultural residues. J Anal Appl Pyrol 2010;88:117–23.